



Extended summary

Rescue of buried people: an electromagnetic model for a feasibility study and system design

Curriculum: Elettromagnetismo e Bioingegneria

Author

Ing. Alfredo De Leo

Tutor(s)

Prof. Graziano Cerri

Date: 15-01-2014

Abstract. The aim of this work is to highlight the paramount importance of the availability of an electromagnetic model for the design of a system based on electromagnetic radiation for search and rescue operation of humans buried under different materials as debris, and snow slide. In this thesis the monitoring of the breathing activity of a man buried into a homogeneous lossy medium has been analyzed. The geometries of the scenario and the body have been simplified in order to model the electromagnetic problem of the interaction of the body and impinging field in a closed-form. In spite of the simple formulation the results are satisfactory and show how some a priori important system requirements can be obtained, as for example the most suitable working frequency range. The model is able to predict the sensitiveness in terms of phase and module variations depending on the scenario.

At first the model is based on plane wave illumination of a human thorax, and then the whole body is introduced: this model was validated by numerical simulation.

Afterwards in order to get a more realistic scenario the plane wave illumination was replaced with a realistic antenna, and the model prediction was confirmed by experimental results.

The model was validated both numerically and experimentally.

Thanks to the analytical model prediction, a prototype of an electromagnetic system to detect the breathing frequency was built up with laboratory equipment, and used both in laboratory and in a realistic scenario.

These measurements showed the feasibility of an electromagnetic victim rescue system, and its ability to detect the respiratory activity during a simulation of a victim in a real scenario, where a victim was buried by excavated soil in a road construction site.

Keywords. breathing detection, rescue systems, CW radar, UWB radar, concealed targets.

1 Introduction

Detection of life signs of human beings with electromagnetic systems is based on movement detection. Heart beating and respiratory motions cause changes in frequency, phase, amplitude, and arrival time of an electromagnetic wave reflected by a human being. Based on these features different radar systems have been developed, that can be grouped into two main families, Doppler radars and UWB systems.

Historically, Doppler systems for the detection of vital signs were first analysed. They are based on the transmission of a signal toward a target region, and on the analysis of the phase changes in the reflected waves, indicating target movements. These movements can be very small, as those caused heart beat and respiration. Transmissions are generally single frequency, and the phase variation due a displacement is proportional to the signal frequency. [1-4].

More recent papers are essentially addressed to overcome existing difficulties for applications to realistic environments, introducing effective processing strategies [5-7]. Over the last few years, radars transmitting ultra-short pulses with an ultra-wide band (UWB) have been also developed. [8-9].

As concerns the search and rescue of earthquake trapped victims, the scenario is extremely complex, the background clutter, including interference due the physiological activity of the operators, has to be accurately analysed and cancelled from the useful signals. [10-12].

In spite of many papers dealing with this topic, it is interesting to note the lack in the literature of an electromagnetic model to describe the scenario in terms of coupling between an impinging wave and a buried body, thus providing important information for the design of a system for locating victims. In this paper we would like to show that even a simplified model can be significant to optimize some parameters. The well-known Green's Integral will be used to describe backscattering of a man, buried into a homogeneous and lossy medium, illuminated by a plane wave. The analytical results will be compared to the numerical simulation, and once validated, will be used to get information on the most suitable frequency range to use as a function of the scenario, that vary in terms of electric property of the medium and position of the victim.

2 Analytical description of the radiation

At first, in order to describe the model, a parallelepiped made by an homogeneous, non magnetic material characterized by an electric conductivity σ_2 , an electrical permittivity ϵ_2 , surrounded by another homogeneous material having dielectric characteristics σ_1, ϵ_1 and illuminated by a plane wave traveling in z direction, and polarized in y -direction is considered.

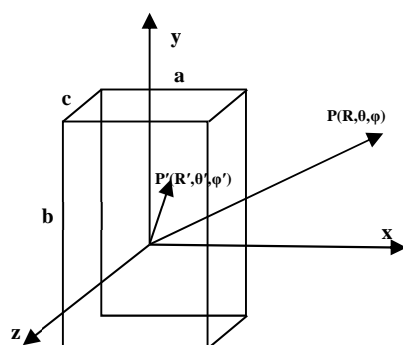


Figure 1.

Simplified model of an human thorax illuminated by a plane wave



In order to have a closed-form of the scattered field, far field condition is assumed.

The field scattered by the object can be evaluated through the equivalent current \vec{J}_{eq}

$$\vec{J}_{eq} = ((\sigma_2 - \sigma_1) + j\omega(\epsilon_2 - \epsilon_1))\vec{E}_2 \quad (1)$$

E_2 being the total electric field inside the body. In general the solution of the electromagnetic problem to evaluate E_2 , performed both with integral methods and Finite Difference Techniques, requires large computational effort. Since the aim of the work is not this specific issue, but the description of the achievable information, a simplified model has been considered.

In this way in the whole volume the well-known formula for the vector potential becomes

$$\vec{A}(\mathbf{R}) = \frac{\mu}{4\pi R} \iiint_V \vec{J}_{eq} e^{-j(\beta_{1x}(x-x') + \beta_{1y}(y-y') + \beta_{1z}(z-z'))} dV \quad (2)$$

A uniform current distribution is adopted in the object side radiated by the impinging wave, and decreasing along z direction because of dielectric losses, according to

$$\vec{J}_{eq} = J_{eq}(z=0) e^{-\alpha_2 z} \vec{y} \quad (3)$$

In this case the equivalent current distribution can be assimilated to a constant current distribution due to an average E field,

$$\vec{E}_{2av} = \frac{1}{\alpha_2 c} \vec{E}_{20} (1 - e^{-\alpha_2 c}) \quad (4)$$

where E_{20} represents the E field maximum value at $z=0$.

The internal field is related to the incident wave by the standard plane wave transmission coefficient

$$E_2 = E_1 \frac{2\eta_2}{\eta_2 + \eta_1} \quad (5)$$

Application of standard expressions allows us to obtain from (2) in a closed form the scattered field

$$\vec{E}(\mathbf{R}, \theta) = -\frac{j\omega\mu}{4\pi R} ((\sigma_2 - \sigma_1) + j\omega(\epsilon_2 - \epsilon_1)) \vec{E}_{2av} e^{-j\vec{\beta}_1 \cdot \vec{R}} e^{-\alpha_1 R} abc \operatorname{sinc}\left(\frac{\beta_{1x} a}{2}\right) \operatorname{sinc}\left(\frac{\beta_{1y} b}{2}\right) \operatorname{sinc}\left(\frac{\beta_{1z} c}{2}\right) \quad (6)$$

α_1, β_1 being attenuation and propagation constant of the surrounding medium respectively.

The simplified model has been validated by the comparison to the result of numerical full wave solution performed by CST Microwave Studio: the backscattered E field evaluated using the analytical expression (6) was compared to the result of the numerical simulation as shown in Fig.2.

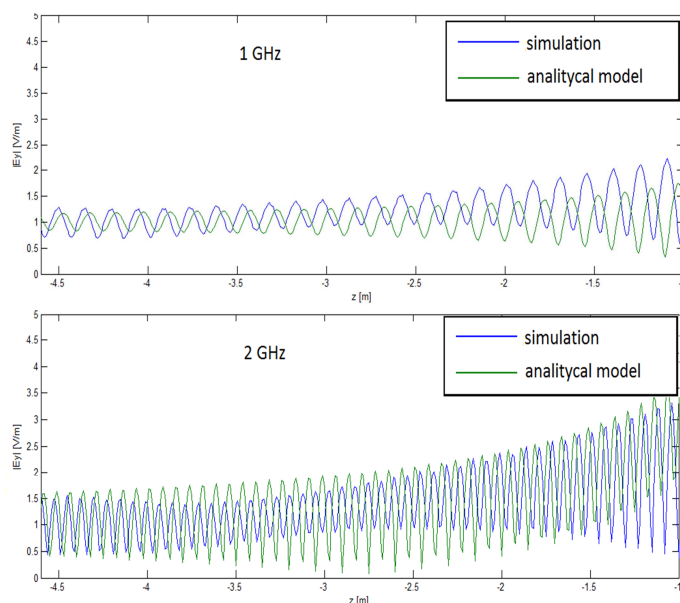


Figure 2. Comparison between numerical simulation and analytical model for a re-radiated electric field of an human chest 400x600x200 mm illuminated by at 1 GHz (above) and at 2 GHz (below) plane wave with $|E| = 1\text{V/m}$

In the coordinate system shown in Fig. 1, the values of $a = 600\text{ mm}$, $b = 400\text{ mm}$, and $c = 200\text{ mm}$ have been chosen, to make this parallelepiped similar to an human thorax, and it was illuminated by a plane wave that travels in free space, in the direction z with a linear polarization with E directed along y , with a maximum intensity of 1 V/m . For human body the values $\epsilon_2 = 70$ and $\sigma_2 = 1\text{ S/m}$ have been chosen.

Even if the model is very simplified, it gives a good level of prediction of the re-radiated E field in the far field zone, according to the assumptions.

3 Electromagnetic Model for the illumination by an aperture antenna

At first, let's describe the human thorax as a parallelepiped made by a homogeneous material characterized by an electric conductivity σ_2 , an electrical permittivity ϵ_2 , surrounded by another homogeneous material having electric characteristics (σ_1, ϵ_1) . The antenna is modeled as an aperture antenna and the axis origin is placed in the center of the aperture, as shown in Fig. 3

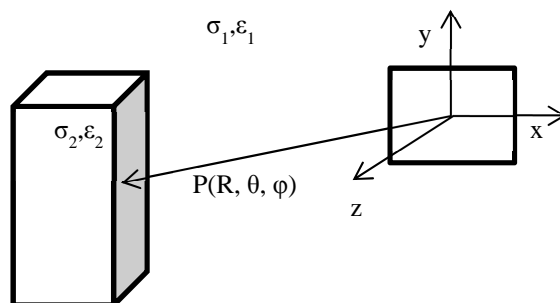


Figure 3. Scenario for the human thorax illuminated by an aperture antenna

The aim of this section is to predict the variation of the reflection coefficient s_{11} measured at the port representing the generator feeding the antenna in function of the variation of the z dimension of the thorax during a respiratory act.

Let's consider a voltage generator (V_g, Z_g) that feeds the antenna having an input impedance equal to Z_{ant} , through the transmission line has a characteristic impedance equal to Z_0 . Assuming the impedance matching between the generator and the transmission line, the average power radiated by the aperture antenna is described by equation (6)

$$W_{rad} = \frac{V_g}{8Z_0} (1 - |\Gamma_{ant}|^2) = \frac{abE_0}{2\eta_1} \quad (7)$$

Where the Γ_{ant} is the complex reflection coefficient of the antenna and η_1 is the wave impedance in medium (σ_1, ϵ_1) . The electric field is backscattered by the thorax towards the antenna and the output voltage V_{out} is

$$V_{out} = \vec{E} \cdot \vec{l}_{eff} \frac{Z_0}{Z_0 + Z_{ant}} \quad (8)$$

Where E_y is the y component of the backscattered electric field at the center of the antenna, and l_{eff} is the effective length of the aperture antenna

$$\vec{l}_{eff} = \sqrt{\frac{4Z_0 ab}{\eta_1}} \hat{z} \quad (9)$$

The reflection coefficient s_{11} can be written as:

$$s_{11} = \frac{E_y l_{eff}}{V_g} \frac{Z_g + Z_0}{Z_0 + Z_{ant}} + \Gamma_{ant} \quad (10)$$

Equation (9) predicts how the complex reflection coefficient varies in function on the scenario; Let's consider the simplified model of a human body represented in Fig. 5, where the grey part of the thorax varies its thickness due to the respiratory movement.

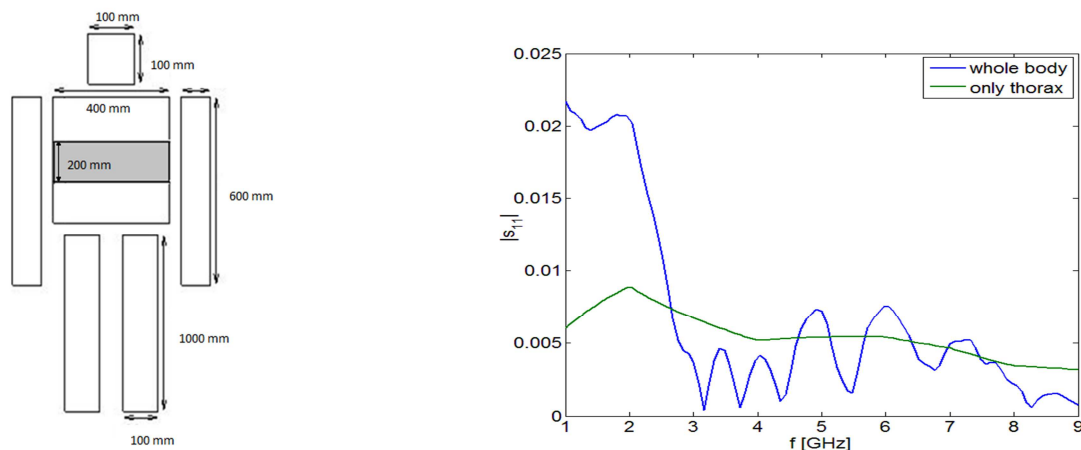


Figure 4. On the left, the human body model; the grey color indicates the part of the body that varies its thickness during a respiratory act. On the right, the comparison of the S_{11} values between human body and thorax backscattering



In S_{11} module prediction let's assume the body motionless with the grey part aligned with the other parts of the thorax.

An aperture antenna with $a=150$ mm and $b=100$ mm placed at 3 meters of distance, with the x and y coordinates centered into the thorax. The surrounding medium is the air ($\epsilon_{r1} = 1$ and $\sigma_2= 0$ S/m) and the human body is made by a lossy dielectric having ($\epsilon_{r2} = 70$ and $\sigma_2= 1$ S/m).

In Fig. 5 is reported the comparison of the S_{11} module variation due to the thorax backscattering and the one due to the whole body. It can be observed that the frequency range from 1 to 2 GHz allows the system to have the maximum sensitiveness in amplitude. It can also be noticed that at lower frequencies the whole body reflects more electric field than the only thorax, whereas at upper frequencies the contributions related to the other parts of the body combine their scattered field in opposition of phase.

The combination of the electric field backscattered from all the parts of the body is so that for certain frequencies the module of the reflection coefficient has a minimum. The values of these frequencies depend on the scenario (distance and direction between the antenna and the victim) but also depend on the impedance matching between the antenna and the generator.

The unpredictability of the scenario suggests that in order to avoid the worst case a frequency sweep analysis is preferable than a traditional continuous wave based system.

4 Experimental Measurement

In last section it was shown that of the analytical model predicts the following a priori system specifications: the best frequency range is from 1 to 2 GHz, the operating mode is the frequency sweep analysis and the antenna would be well matched to reduce the second addendum in equation (10).

In this first experimental measurements an anechoic scenario was implemented to better validate module and phase prediction. Subsequently the breathing frequency was measured, at first in a realistic lossless scenario, and then introducing dissipative elements.

4.1 Model Validation

The following experimental setup, shown in Fig. 7, was built on to validate the analytical model: a broadband antenna (Double Ridge Horn Antenna) connected to a Vectorial Network Analyzer (VNA) was positioned at a distance $D = 3$ m from the obstacle placed in an anechoic angle and a PC acquired the VNA measurements and stored them an offline elaboration. The obstacle, that represented an human thorax, was a 400 mm x 400 mm x 50 mm Plexiglas box filled with salted water. The VNA performs a frequency sweep from 1 to 9 GHz, because this is the maximum range available using both the VNA calibration kit and the antenna. The antenna impedance was measured at all the frequency used for the simulations, and these values used in the analytical model.

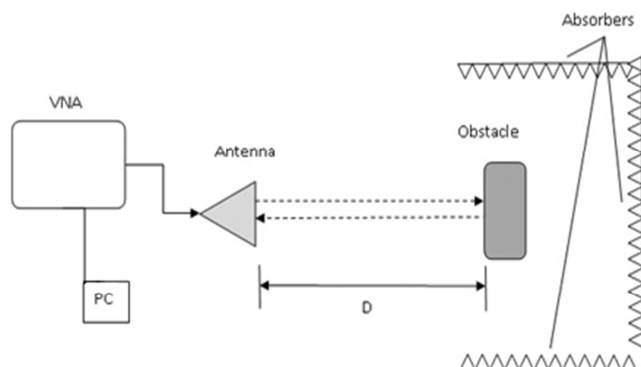


Figure 5. Experimental setup in anechoic environment

In Fig. 8 is reported the comparison between the measurement and the model prediction; the big discrepancy at $f = 1$ GHz and $f = 9$ GHz, is due to the Time Gate function activated into the VNA to isolate the pulse related to the first thorax reflection.

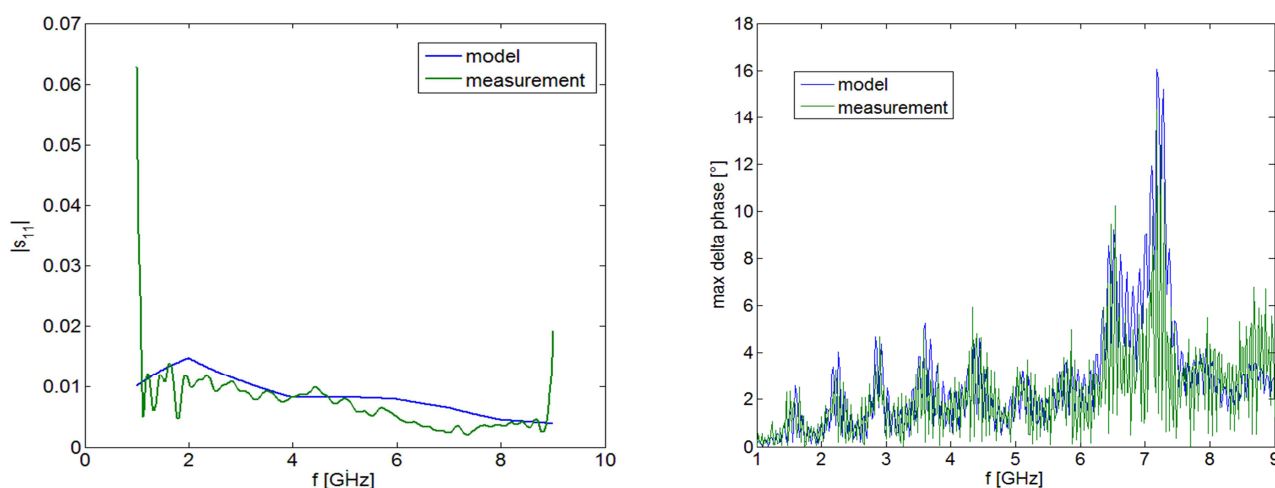


Figure 6. Comparison between the model prediction and the measurement for the module and phase of the reflection coefficient

From the comparison of these two curves emerges that there is an appreciable level of agreement between the prediction of the model and the measurement results.

4.2 Breathing Detection

Once validated the model and built up a system prototype using laboratory instrumentation thanks to the system a priori specifications, such prototype was used to detect the breathing frequency of a concealed target. As shown in Fig. 8, a human being was placed lying on the floor, and the antenna, hanged up by a dielectric structure at the height of 2 meters. The antenna was placed so that the electric field was parallel to the main

dimension of the man. The first measurement was carried on free space, then in order to simulate the losses of the medium that surrounds the victim, in each of the three next measurement an absorbing panel was added, placing it above the victim. It can be experimentally estimated that the insertion of three absorbing panel introduces an attenuation of about 20 dB. The electrical conductivity and permittivity of that soil depends mainly on the its water content, therefore it can be estimated that 20 dB of attenuation corresponds to a 5 m of depth in case of dry soul, whereas as the water percentage increases as well the maximum detectable distance decreases, but on the other hand also the probability that the victim is still alive decreases. It must be remarked that the proposed electromagnetic system senses the presence of a victim buried into rubbles through the measurement of its breathing activities, and so a dead person is not detectable. This feature may be useful if more than one person buried in a catastrophic event, to direct the research of those still alive. For this reason in breathing detection measurement, the respiratory frequency is the main parameter to identify, while the other harmonics are less significant.

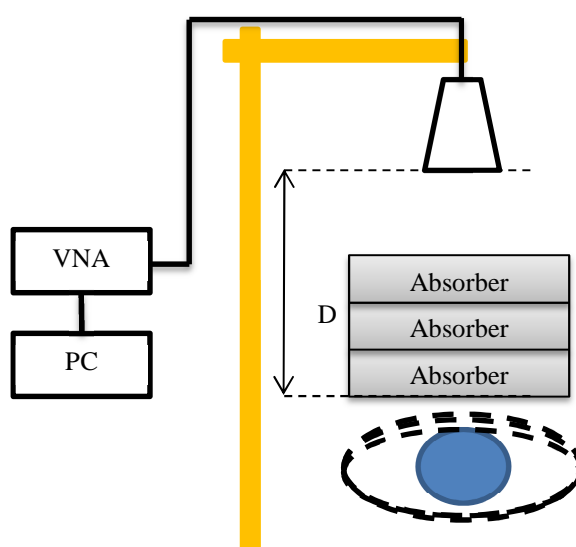


Figure 7. Experimental setup for breathing measurement

The PC connected to the VNA stores the complex reflection coefficient each frequency scan, that varies from 1 to 2 GHz, performing the measurement in $N=71$ equidistant points. Each scan stands for 340 ms, and 120 scans are acquired for a total measuring time of about 40 s; in this way a matrix of values $S_{11}(t_i, f_j)$ is stored into the PC memory, where t_i ($i=1..120$) represents the acquisition time and f_j ($j = 1..71$) represents the frequency point where the measurement is performed.

Each column of the $S_{11}(t_i, f_j)$ represents the time variation of the complex reflection coefficient, measured at a certain frequency; performing a Fourier Transform on each column values, the s_{11} frequency spectra are obtained. Subsequently all the spectra are averaged to have a unique reconstructed signal spectrum, where the breathing frequency and its harmonics can be detected.

Fig. 9 reports these reconstructed spectra when none, one, two or three absorbing panel are inserted.

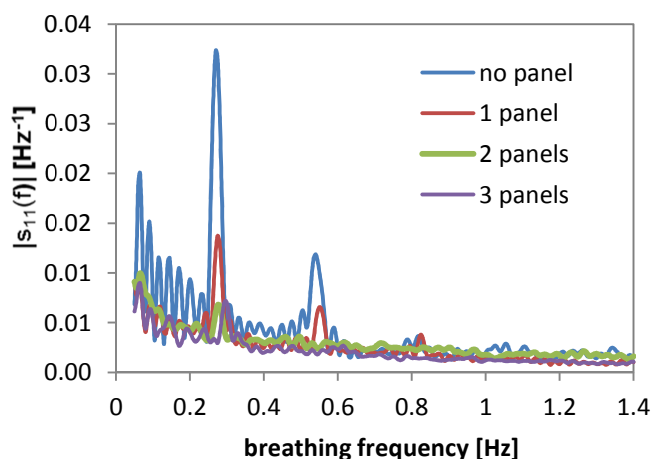


Figure 8. Fig. 9. Measured breathing frequency

It can be observed that the sensed breathing frequency is about $f_{res} = 2.5$ Hz; this frequency can be detected also when all the three absorbing panels are inserted, even if the amplitude of the harmonics decreases while the losses increase. The lower part of the spectrum represents the effect of the very slow and not related to the respiration movement of the body during the 40 seconds of the measurement.

5 Conclusions

In current work the feasibility of a rescue system based on RF radiation, able to detect the breathing activities, in particular the respiratory frequency, was investigated.

In spite of the availability of many researches that present electromagnetics systems based on Radio Doppler or UWB, it emerged the lack of an analytical model, useful to predict some important a priori design parameters, mainly the choice between a continuous wave and a pulse system.

This choice would be done using one of the available electromagnetic simulators, but they all need a full wave solution by a burden numerical tool, so necessitating the use of a supercomputer due to the big amount of memory, CPU and computational time required.

On the other hand an analytical model would require some approximations to solve the integral and differential equations: each approximation introduced has been motivated and validated by numerical simulation or experimental measurement.

In particular the numerical simulation was helpful to validate the model in case of plane wave illumination, due to the lack an anechoic environment in our laboratory where perform the test.

Once validated the model, it was used to predict some important a priori design parameter: the non-perfect impedance matching between the antenna and the RF source and the multiple reflection of the surrounding environment cause a phenomenon of destructive interference at certain frequencies, and such frequencies are unpredictable: for this reason a frequency sweep based system was taken in consideration.

The model predicts also the frequency range in which the electromagnetic system has the maximum sensitivity and the maximum distance at which the victim respiration can be detected.

Using all these design parameters predicted by the model, a prototype was built up using the instrumentation in our laboratories, in particular a Vectorial Network Analyzer, a Double Ridge horn antenna and a laptop for the offline signal processing.



With this system a set of measurements in a controlled environment was carried on to validate the model and to detect the breathing activity in both lossless and lossy scenario.

Possible future developments may be the characterization of more complex and realistic environments through a statistical analysis, such as in the case of an avalanche where the snow can be still approximated to a homogeneous lossy medium, but the presence of rocks or tree trunks can create clutter, and then furtherly degrade system performances.

Another improvement would be the real time breathing frequency detection, and the implementation of this software directly into the VNA, increasing in this wave both the portability and the efficiency.

The final step would be the realization of a prototype using a dedicated hardware: in this wave the costs would be reduced, and the maximum output power would increase and so the maximum distance at which the victim breathing frequency could be detected.

6 References

- [1] V. M. Lubecke, O. B. Lubecke, A. H. Madsen, and A. E. Fathy, "Through the wall Radar Life Detection and Monitoring", Proc of IEEE – IMS, Honolulu, USA, June, 2007, pp.769-772.
- [2] C.I. Franks, B.H. Brown, D.M. Johnston, "Contactless respiration monitoring of infants", Med Biol Eng, vol. 14:3, pp. 306-318, 1976.
- [3] K. M. Chen, D. Misra, H. Wang, H. Ru Chuang, and E. Postov, "An X-band Microwave Life-Detection System", IEEE Trans on BME, vol. 33, No.7, July 1986, pp. 697-701.
- [4] Q. Zhou, J. Liu, A. Host Madsen, O. Boric-Lubecke, and V. Lubecke, "Detection of multiple heartbeats using Doppler Radar", Proc. IEEE ICASSP 2006, pp.1160-1163.
- [5] S. I. Ivashov, V. V. Razevig, A. P. Sheyko, I. A. Vasilyev, "Detection of Human Breathing and Heartbeat by Remote Radar", Progress in Electromagnetic Research Symp., Pisa, Italy, March 28-31, 2004, pp. 663-666.
- [6] C. Li, and J. Lin, "Random Body Movement Cancellation in Doppler Radar Vital Sign Detection", IEEE Trans. on MTT, Vol. 56, No. 12, December 2008, pp.3143-3152.
- [7] M. D'Urso, G. Leone, F. Soldovieri, "A simple Strategy for Life Signs Detection via an X-Band Experimental Set-up", Progress in Electromagnetic Research C, vol.9, 2009, pp.119-129.
- [8] A. G. Yarovoy, L. P. Ligthart, J. Matuzas, and B. Levitas, "UWB Radar for Human Being Detection", IEEE A & E Systems Magazine, March 2006, pp. 10-14.
- [9] A. G. Yarovoy, X. Zhuge, T. G. Savelyev, L. P. Ligthart, "Comparison of UWB Technologies for Human Being Detection with Radar", Proc. Of the 4th European Radar Conf, 2007 EuMA, October 2007, Munich, Germany, pp. 295-298.
- [10] K. M. Chen, Y. Huang, J. Zhang, A. Norman, "Microwave life-Detection Systems for Searching Human Subjects Under Earthquake Rubble or Behind Barrier.
- [11] I. Arai, "Survivor search radar system for persons trapped under earthquake rubble", Proc. of APMC2001, Taipei, Taiwan, pp. 663-668.
- [12] M. Bimpas, K. Nikellis, N. Paraskevopoulos, D. Economou, and N. Uzunoglu, "Development and testing of a detector system for trapped humans in building ruins", 33rd European Microwave Conf, Munich, 2003, pp. 999-1002.